Environmental Pollution 358 (2024) 124515

Contents lists available at ScienceDirect

Environmental Pollution

journal homepage: www.elsevier.com/locate/envpol

Unique impacts of strong and westward-extended western Pacific subtropical high on ozone pollution over eastern China☆

Mengyun Li[a], Yang Yang[a,*], Hailong Wang[b], Pinya Wang[a], Hong Liao[a]

[a] Joint International Research Laboratory of Climate and Environment Change, Jiangsu Key Laboratory of Atmospheric Environment Monitoring and Pollution Control, Jiangsu Collaborative Innovation Center of Atmospheric Environment and Equipment Technology, School of Environmental Science and Engineering, Nanjing University of Information Science and Technology, Nanjing, Jiangsu, China

[b] Atmospheric, Climate, and Earth Sciences Division, Pacific Northwest National Laboratory, Richland, WA, USA

ARTICLE INFO

Keywords:
WPSH
Ozone pollution
Meteorological fields
GEOS-Chem

ABSTRACT

As a subtropical anticyclonic high-pressure system that typically forms over the northwestern Pacific Ocean in summer, the Western Pacific subtropical high (WPSH) affects meteorological conditions and ozone pollution in China. The relationship between maximum daily 8-h average ozone (MDA8 O_3) concentrations and the extremely strong and westward-extended WPSH occurred in 2022 is investigated using observations, reanalysis data and atmospheric chemistry model simulations. During July–August 2022, a significant positive relationship existed between the intensity of the WPSH and MDA8 O_3 over southern China, with a correlation coefficient of +0.44, but the correlation is negative (−0.40) in northern China. During the strong WPSH days, MDA8 O_3 increased by 16.5 μg m^{-3} (16.4% relative to July–August average) over southern China and decreased by 19.0 μg m^{-3} (14.5%) in northern China compared to the weak WPSH days. The unique dipole pattern in the relationship between ozone levels and the WPSH in 2022 exhibited a contrast to that during 2015–2021. The difference is primarily due to the extremely strong WPSH intensity and its unusual westward expansion in 2022. In this case, an anomalous anticyclone at 500 hPa dominates over southern China, which creates conditions conducive for ozone formation and accumulation. The anticyclone weakened horizontal winds and reduced the dispersion of ozone, alongside a high temperature and low relative humidity, which favored the chemical production of ozone. In contrast, abnormal northerly winds enhanced ozone diffusion in northern China and the low temperature reduced ozone chemical production. This study reveals the mechanism for the significant impact of strong and westward-extended WPSH on ozone concentrations over China, emphasizing the role of the WPSH location in modulating meteorology and ozone levels.

1. Introduction

Ozone pollution in China has drawn increasing attention in recent years, due to its great effects on ecosystem function, social economy and human health (Yao et al., 2022; Feng et al., 2021; Li et al., 2022; P. Wang et al., 2022). Ozone pollution is still a major issue, despite China's recent implementation of a number of preventive and control measures against air pollutants (Li et al., 2020; Liu and Wang, 2020; Ni et al., 2024; Shen et al., 2022). Meteorological conditions significantly influence tropospheric ozone concentrations by modulating natural emissions rates, transport, accumulation, and chemical formation processes of ozone (Ding et al., 2023; H. Li et al., 2023; M. Li et al., 2023; Lyu et al., 2019; Sahu et al., 2021; Zhu et al., 2024). For example, by using a chemical transport model (GEOS-Chem), Dang et al. (2021) found that changes in meteorological conditions could explain 49% and 84% of the increases in maximum daily 8-h average ozone (MDA8 O_3) concentrations in North China Plain (NCP) and Yangtze River Delta (YRD), respectively, during 2012–2017.

Variation in large-scale circulation patterns can modulate the meteorological conditions that are critical to ozone pollution (Shi et al., 2020; Wang et al., 2022; Yang et al., 2022, 2024; Zhou et al., 2022). According to Dong et al. (2020), there is a tendency for severe ozone pollution in the NCP region due to a low-pressure center in northeastern China and an anomalous high-pressure over the North Pacific. Hu et al.

☆ This paper has been recommended for acceptance by Prof. Pavlos Kassomenos.

* Corresponding author.
E-mail address: yang.yang@nuist.edu.cn (Y. Yang).

https://doi.org/10.1016/j.envpol.2024.124515
Received 2 May 2024; Received in revised form 13 June 2024; Accepted 7 July 2024
Available online 10 July 2024

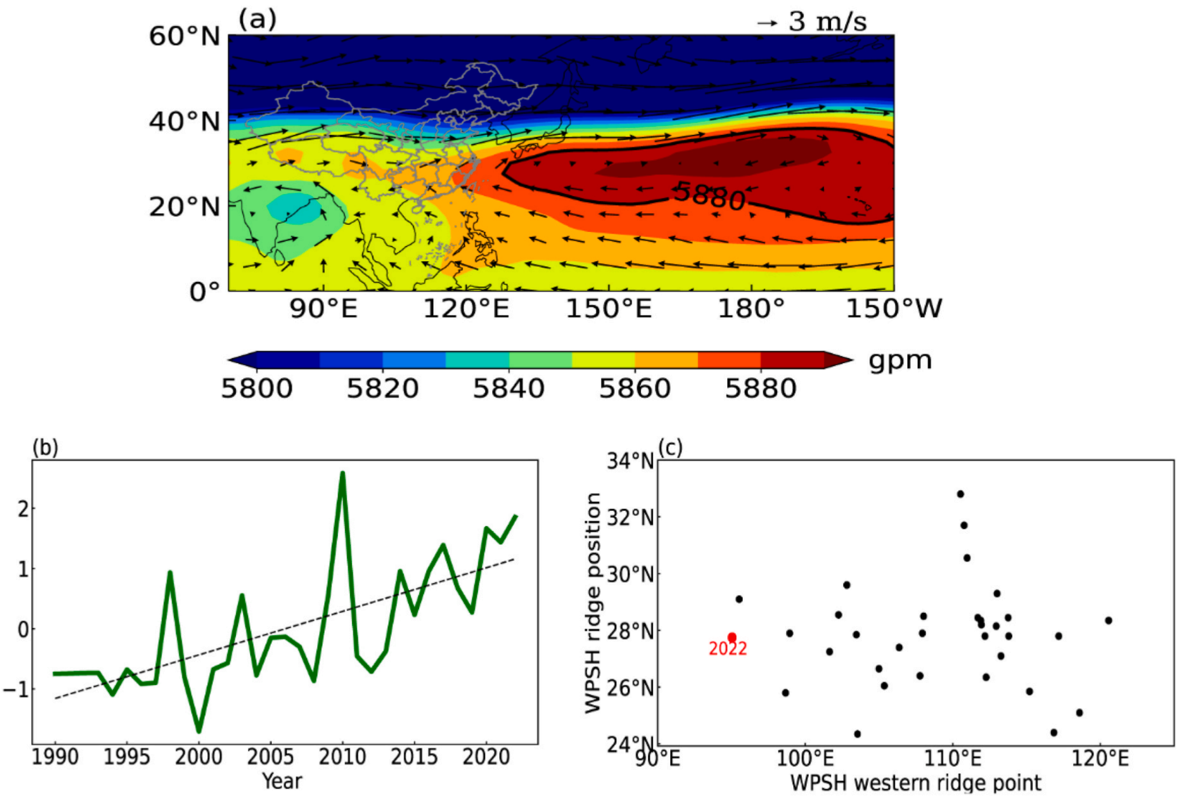

Fig. 1. (a) The climatological mean of July–August geopotential height (contour, gpm) and wind fields (m s^{-1}) at 500 hPa during 1990–2021. (b) Time series of the standardized intensity of WPSH index (WPSH–I) over 1990–2022. (c) Scatter diagram of WPSH position. The solid line in (a) denotes 500 hPa geopotential height at 5880 gpm. The dashed line in (b) indicates the linear trend of WPSH-I. The horizontal axis in (c) represents the longitude of westward ridge point of WPSH (WPSH–W) for each year in July–August, the vertical axis represents the ridge line of WPSH (the latitude location of the isoline inside the geopotential height contour of 5880 gpm with 500 hPa zonal wind $u = 0$ and $\partial u/\partial y > 0$), and red dot marks the location for 2022. (For interpretation of the references to colour in this figure legend, the reader is referred to the Web version of this article.)

(2024) showed that high ozone episodes occurred in China were often associated with the Western Pacific subtropical high (WPSH), which can affect the formation and transport/accumulation of ozone. Therefore, it is particularly important to explore the influence of large-scale circulation systems (e.g., WPSH) on ozone pollution, which can be useful for air quality monitoring, forecasting, and assessment.

The WPSH is a dominant atmospheric high-pressure system that typically forms over the northwestern Pacific Ocean in summer and is a significant component of the global atmospheric circulation system (Wu and Zhou, 2008; Zhang et al., 2022). It brings stable, dry weather to areas beneath it and plays an important role in influencing regional weather patterns. The variations in the intensity, shape, and location of the WPSH show its associated complex seasonal variability. In summer, the WPSH reaches its peaking phase and has a considerable impact on weather and climate in East Asia (Choi and Kim, 2019; Qi et al., 2010; Zhou, 2005; R. Wang et al., 2023), which can further affect the budget processes of air pollutants there. Many studies have examined the effects of the WPSH on ozone pollution in China (Chang et al., 2019; He et al., 2012; Lo and Hung, 2015; Jiang et al., 2020). The change in dominant spatial patterns of summertime surface ozone in eastern China was closely related to WPSH during the 2015 to 2019 (Yin and Ma, 2020). Chang et al. (2019) found that the meteorological conditions in Shanghai caused by the strong WPSH in July 2016 were conducive to the photochemical formation of ozone and increases in ozone concentrations compared with a weak WPSH scenario. Based on observations in 2014, Zhao and Wang (2017) found that a strengthened WPSH could induce stronger southerly winds, enhancing moisture transport to southern China and causing more precipitation, lower temperatures, and less UV radiation, which led to decreases in ozone concentrations over southern China. Meanwhile, depleted water vapor resulted in dry and sunny weather conditions, favoring ozone formation and therefore increasing ozone concentration in North China during the strengthened WPSH days.

During July–August 2022, the Northern Hemisphere endured an extremely hot summer, marked by record-breaking temperatures in eastern China. X. Li et al. (2023) pointed out that the strengthened and westward expanded WPSH led to a reduced cloud cover and an increased downward shortwave radiation at the surface, which resulted in the record heatwave in 2022. Thus , the anomalously strong and westward extended WPSH in 2022 has drawn attention due to its significant impact on weather patterns (Ma et al., 2023). The WPSH extended westward due to a descending Rossby wave over the western North Pacific (Tang et al., 2023) and caused the dominance of anomalous high pressure over East Asia (Tan et al., 2023; Zhao et al., 2023). Y. Wang et al. (2023) found that the anomalous descending motion associated with WPSH significantly suppressed local precipitation, leading to the extreme drought over YRD in 2022. Overall, the meteorological conditions during July–August 2022 were largely regulated by the extremely strong and westward-extended WPSH, which likely had significantly different influences on the ozone pollution over China compared to normal ones.

The objective of this study is to examine the influence of the unusual 2022 WPSH on the variability of ozone concentrations in China. Subsequently, the possible mechanisms of the impacts of the extreme WPSH on near-surface ozone levels are investigated though analyzing the meteorological conditions from meteorological reanalysis products and by assessing the physiochemical processes with GEOS-Chem model experiments. We aim to provide useful insights into the causes of ozone pollution under the unique synoptical conditions and improve the predictability of ozone levels in China, which can aid in developing future

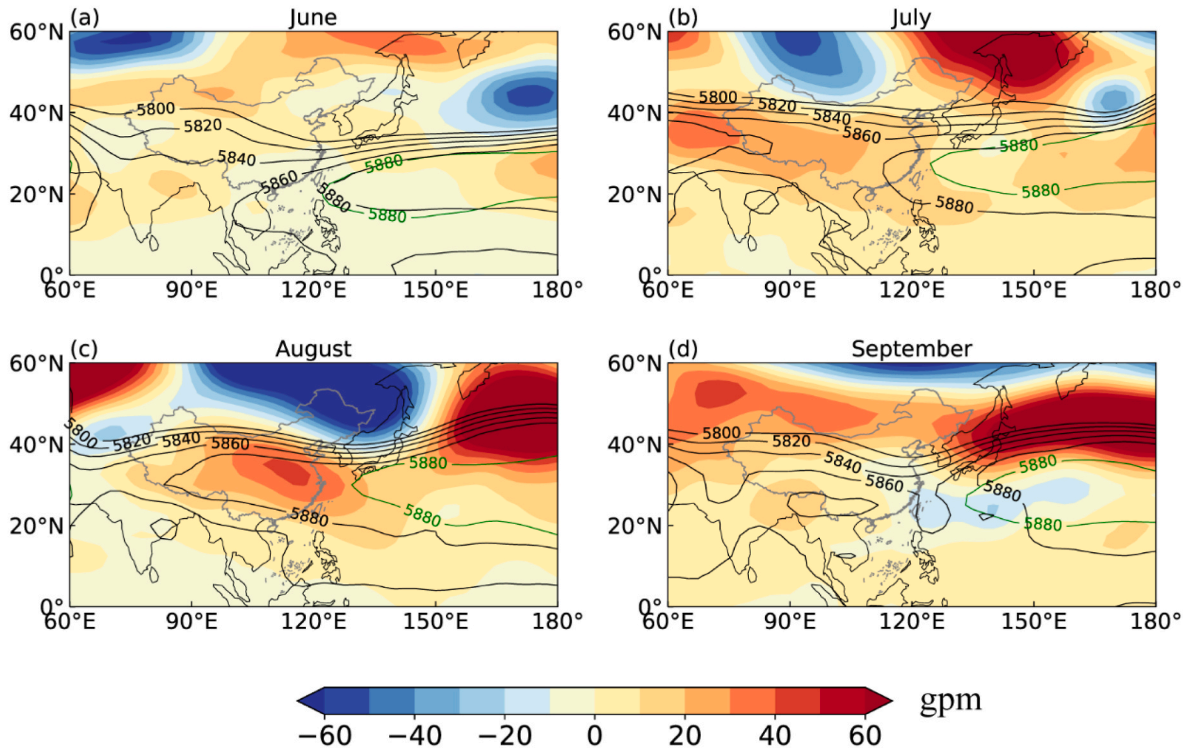

Fig. 2. The monthly mean geopotential height (black lines, units: gpm) at 500 hPa in 2022 for (a) June, (b) July, (c) August and (d) September and their anomalies (contour) relative to the corresponding climatological mean (1990–2021). The green lines represent climatological mean geopotential height at 5880 gpm for the corresponding month. (For interpretation of the references to colour in this figure legend, the reader is referred to the Web version of this article.)

ozone control measures.

2. Data and methods

2.1. Ozone observations

The China National Environmental Monitoring Centre (CNEMC, https://quotsoft.net/air/) provides nationwide ground-level hourly ozone concentration data since 2013, which have been used in many previous studies (Gao et al., 2020; Ye et al., 2024). The sites with consecutive observations from 2015 to 2022 are selected for analysis. In this study, the MDA8 O_3 concentrations are used to assess ozone air quality. We focus on the impacts of extreme WPSH on ozone concentrations over eastern China during July–August, considering that the remarkable ozone pollution usually happens in these months (Zong et al., 2021).

According to the observed MDA8 O_3, areas over eastern China suffered from serious ozone pollution in July–August from 2015 to 2022, including southern China (20°–32°N, 107.5°–120°E) and northern China (32°–44°N, 107.5°–120°E). The regional averaged MDA8 O_3 was as high as 135 μg m^{-3} in northern China and 98 μg m^{-3} in southern China (Fig. S1). Meanwhile, the high standard deviation of the daily MDA8 O_3 concentrations indicates that near-surface ozone levels have a strong daily variability, which can be linked to the meteorological conditions (Han et al., 2020).

2.2. Model simulations

The ozone concentrations are simulated in this study using a nested global atmospheric chemistry model GEOS-Chem Version 13.4.1, which has been applied to a variety of air pollution-related scientific fields (Colombi et al., 2022; David et al., 2019; Li et al., 2019). The nested experiments are conducted at a horizontal resolution of 0.5° × 0.625° (latitude × longitude) for the years 2015–2022 (see Text S1 for details of the model and simulation). GEOS-Chem also employs an advanced diagnostics package to estimate species gross production/loss, which decomposes the changes in species into individual process contributions (Gong and Liao, 2019; X. Li et al., 2023; Lin and McElroy, 2010). It is employed in this study to determine the relative impact of important chemical and physical processes on net changes in ozone concentrations.

The performance of the GEOS-Chem model in replicating observed ozone concentrations across China is assessed and shown in Fig. S2. The ozone concentrations are assessed in 2019 since during simulations, anthropogenic emissions are fixed at that year. The GEOS-Chem model can realistically reproduce the spatial distributions of MDA8 O_3, with a spatial correlation coefficient (R) up to +0.8 ($p < 0.01$) between the simulated and the observed MDA8 O_3 for July–August in 2019 (Fig. S2a). The simulated MDA8 O_3 concentration is slightly higher than the observed value, with a normalized mean bias (NMB) of 20%. The GEOS-Chem successfully captures the daily variability of MDA8 O_3 during July–August over China, with more than 80% of the sites showing a statistically significant positive correlation ($R > 0.32$, $p < 0.01$) between the observed and simulated daily MDA8 O_3 (Fig. S2b). These results demonstrate that the GEOS-Chem model is capable of effectively capturing the daily variations and spatial distribution of ozone levels in China during July–August.

2.3. The WPSH index

This study employs the geopotential height at 500 hPa to quantify fluctuations in the WPSH based on NCEP/NCAR reanalysis (https://psl.noaa.gov/data/gridded/data.ncep.reanalysis.html). Two WPSH metrics including intensity index (WPSH–I) and westward expansion ridge point (WPSH–W) are used to assess the intensity and expansion of the WPSH (Chen et al., 2021; Zhang et al., 2022). WPSH-I is calculated as the accumulated geopotential height anomaly enclosed by the 5880 geopotential meters (gpm) at 500 hPa within the region of 110°E to 180°E longitude and extending northward from 10°N latitude. WPSH-W marks the longitude corresponding to the westernmost extent of 5880 gpm

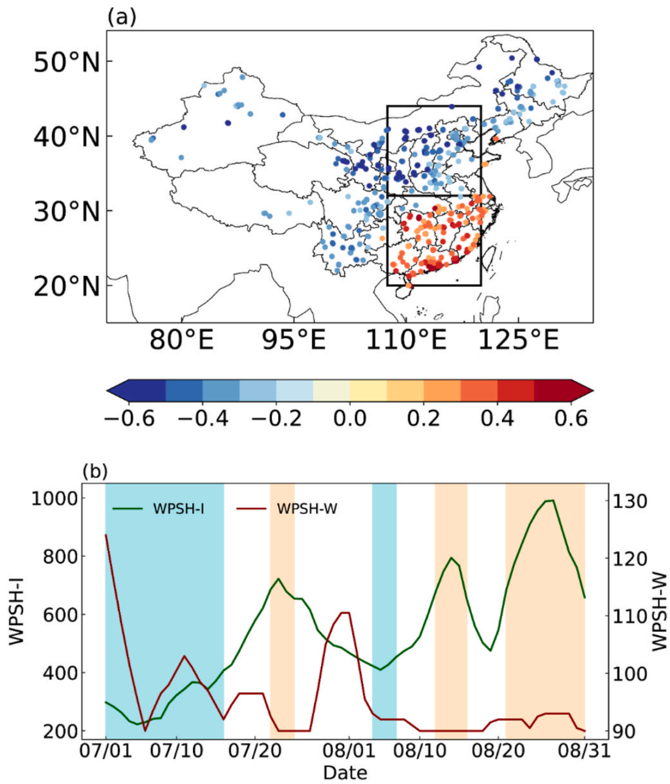

Fig. 3. (a) Spatial distribution of the correlation coefficients between daily MDA8 O_3 concentrations and WPSH-I during July–August 2022. (b) Time series of the WPSH-I and WPSH-W during July–August 2022. Only sites with statistical significance above the 95% confidence level are shown in (a). The boxed area marks northern and southern China. Colored stripes in (b) illustrate the strong (orange) and weak (blue) WPSH days, defined as the highest and lowest 30% WPSH-I days, respectively. (For interpretation of the references to colour in this figure legend, the reader is referred to the Web version of this article.)

contour at 500 hPa over the region between 90°E and 180°E, which represents the relative position of WPSH in the meridional direction. Note that the daily WPSH indices are obtained after taking a 5-day running average (Liu et al., 2022; Keller et al., 2021).

Fig. 1a shows the long-term (1990–2021) average of July–August geopotential height and winds at 500 hPa, highlighting the 5880 gpm contour that delineates the spatial extent of the WPSH. The approximate location of the western ridge point of the WPSH is around 130°E. On the west side of the WPSH, winds shift from southeasterly to southwesterly, which move a large amount of humid air into East Asia (Qu et al., 2013; Wu et al., 2019). The intensity index of WPSH derived from the NCEP/NCAR exhibits a strong correlation with ERA5 reanalysis, with a correlation coefficient of 0.98. The WPSH-I shows a clear upward trend during 1990–2022 (Fig. 1b), consistent with the intensification of WPSH in recent decades (Wu and Wang, 2015; Hong et al., 2023). The WPSH in 2022 was the second strongest one in intensity and had the westernmost location during 1990–2022 (Fig. 1c).

3. Results

3.1. The characteristics of abnormal WPSH in 2022

As a semi-permanent subtropical anticyclonic high-pressure system, WPSH usually reaches its peak intensity in boreal summer (Guan et al., 2019). The monthly 5880 gpm geopotential height at 500 hPa during June–September in 2022 and its corresponding climatological mean (1990–2021), as well as the anomalies in geopotential height, are shown in Fig. 2. In June 2022, the intensity and location of the WPSH are comparable with their climatological mean. Then, it extended westward in July and reached its westernmost location in August. Specifically, the positive geopotential height anomalies cover most of China. The westernmost edge of the 5880 gpm of geopotential height is located around 80°E in August, a shift of 50° westward from the climatological mean. Most of East Asia is dominated by the anomalous high pressure, adjoined by an anomalous low-pressure system over Siberia. Then, the WPSH withdrew eastward in September. In general, WPSH showed anomalous strong intensity and extended coverage westward in July–August of 2022 compared to climatology, which likely impacted ozone air quality in China.

3.2. The relationship between daily MDA8 O_3 and WPSH

During 2015–2021, daily MDA8 O_3 and WPSH-I generally exhibit a negative correlations correlation over southern China, while in northern China, they demonstrated a positive correlation (Fig. S3). It is in good agreement with previous studies, showing that during strong WPSH, the anomalous southerly winds bring clean air from the ocean, causing an increase in relative humidity and a decrease in solar radiation in southern China, and thus surface O_3 concentrations decreased over southern China (Jiang et al., 2020; Zhao and Wang, 2017). The conditions of high temperature, intense solar radiation, and low relative humidity in northern China are conducive to the formation and buildup of surface ozone during the strong WPSH.

However, the relationship in year 2022 with the extremely strong and westward-extended WPSH is much different. Fig. 3a demonstrates the spatial distributions of the correlation coefficients between daily MDA8 O_3 and WPSH-I over China. Over the polluted eastern China (20°–44°N, 107.5°–120°E), where high levels and variability of MDA8 O_3 is located, a distinct dipole pattern of correlation is observed, with significant positive correlations over southern China (+0.44 on average) and negative correlations in northern China (−0.40). The results suggest

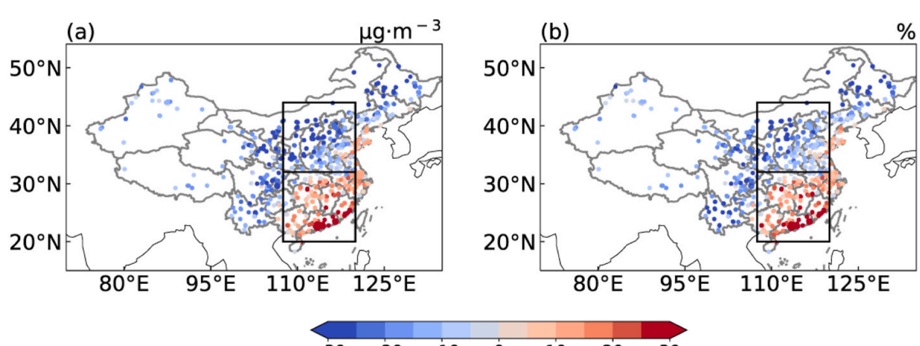

Fig. 4. (a) Absolute ($\mu g \cdot m^{-3}$) and (b) percentage (%, relative to the July–August mean in 2022) difference in the observed MDA8 O_3 concentrations between strong and weak WPSH days during July–August 2022. The boxed area marks northern and southern China.

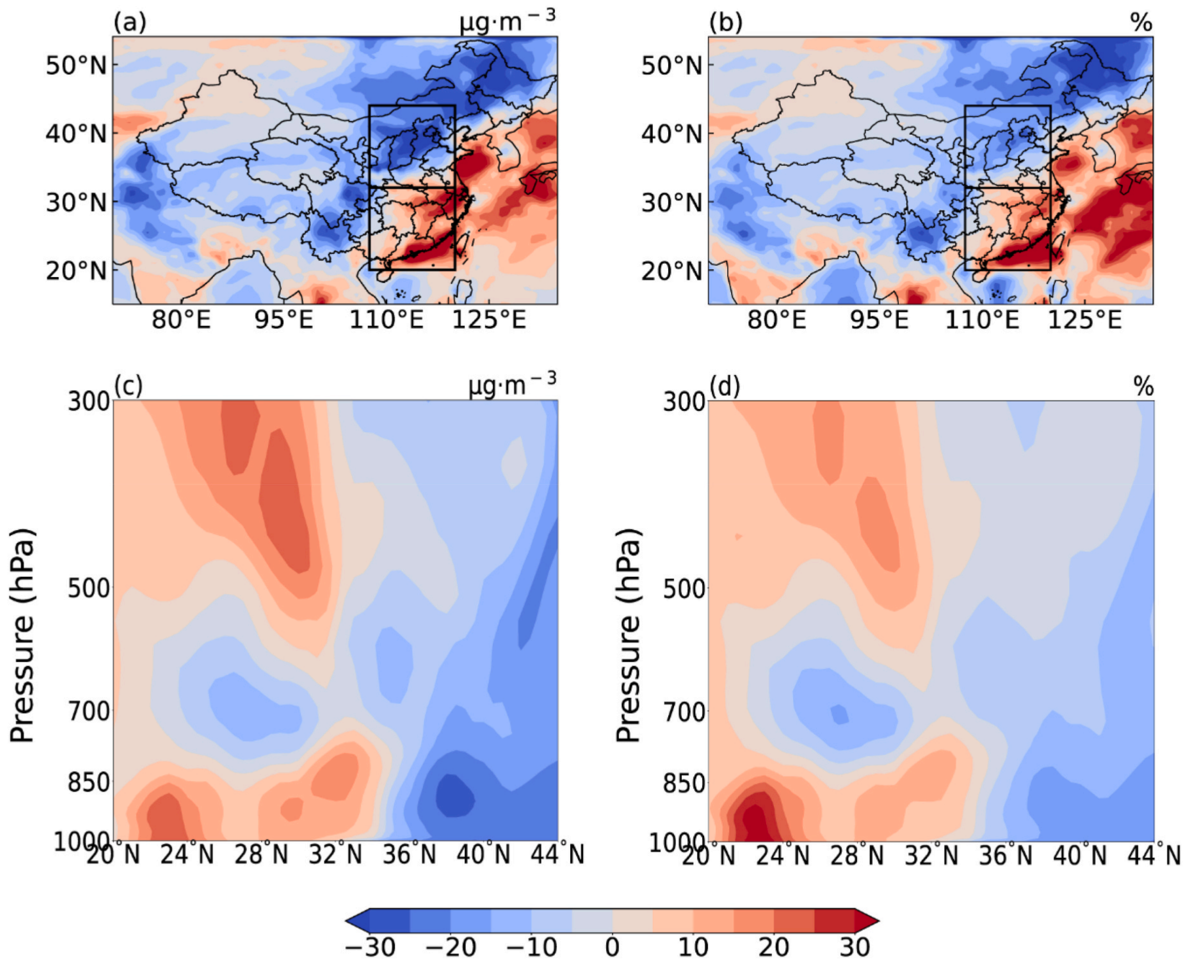

Fig. 5. (a) Absolute ($\mu g \cdot m^{-3}$) and (b) percentage (%, relative to the July–August mean in 2022) difference in the simulated MDA8 O_3 concentrations between strong and weak WPSH days during July–August 2022 from the GEOS-Chem simulations. Pressure-latitude cross sections averaged over 107.5°–120°E for (c) absolute ($\mu g \cdot m^{-3}$) and (d) percentage (%) differences. The boxed area marks northern and southern China.

that the stronger WPSH days in 2022 tend to trigger more heavily ozone pollution events in southern China than the weaker days and vice versa in northern China.

To quantify the effects of WPSH on ozone levels in 2022, Fig. 4 presents the composite differences of MDA8 O_3 between the strong and the weak WPSH days, which are selected by the highest and lowest 30% of WPSH-I days in July–August 2022 shown in Fig. 3b. Consistent with the dipole pattern of correlations between daily MDA8 O_3 and WPSH-I, the composite differences in MDA8 O_3 concentrations over eastern China are generally positive over southern China but negative over northern China between the strong and weak WPSH days. The regional average of observed MDA8 O_3 concentration increases by 16.5 μg m^{-3} (16.4% relative to the July–August mean) in southern China and decreases by 19.0 μg m^{-3} (14.5%) in northern China during the strong WPSH days, compared to the weak WPSH days.

GEOS-Chem model simulations are designed and applied to examine the physiochemical processes underlying the differences of MDA8 O_3 between strong and weak WPSH days. The spatial distribution and pressure-latitude cross-section of the differences in simulated MDA8 O_3 concentrations between the strong and weak WPSH days in 2022 are shown in Fig. 5. In coincidence with observations, southern China experienced positive MDA8 O_3 anomalies with an average of 14.1 μg m^{-3} (13.3%) during strong WPSH days, compared to weak WPSH days, shown in model simulations, whereas northern China showed negative MDA8 O_3 anomalies with an average of −16.7 μg m^{-3} (−11.1%). In addition, this dipole pattern of ozone differences in eastern China between the strong and weak WPSH days are also identified in the vertical profile from the surface up to 800 hPa (Fig. 5c and d).

3.3. *The underlying mechanism of the WPSH impacts on ozone in 2022*

Fig. 6 demonstrates the composite differences in meteorological parameters that mainly affect the horizontal and vertical transport of ozone between the strong and weak WPSH days in 2022 from MERRA-2 reanalysis. The sea level pressure decreases over the Sea of Okhotsk and increases over Mongolia during strong WPSH days, inducing anomalous northerly winds at 850 hPa over eastern China (Fig. 6a). The anomalous northerly wind can move the ozone-rich air from northern China to southern China, resulting in higher ozone in southern China and lower ozone concentrations in northern China during the strong WPSH days than weak WPSH days. Meanwhile, an anomalous anticyclone at 500 hPa dominates over southern China due to the westward extension of WPSH in 2022 (Fig. 6b), causing the region around 30°N to be controlled by a strong subsidence (Fig. 6c). An anomalous cyclone is located over the Sea of Okhotsk, contributing to updraft above north China. These two systems converged around 32°N, resulting in dipole pattern of correlation in south and north China. The anomalous downdraft together with increases in planetary boundary layer height (Fig. 6d) is conducive to the downward dispersion of ozone from the upper layer (H. Liu et al., 2022; Ouyang et al., 2022), thereby contributing to elevated near-surface ozone levels in southern China. The above findings suggest that the changes in horizontal and vertical winds are favorable for ozone accumulation over southern China and ozone dispersion over northern China during the strong WPSH days compared to weak WPSH days in

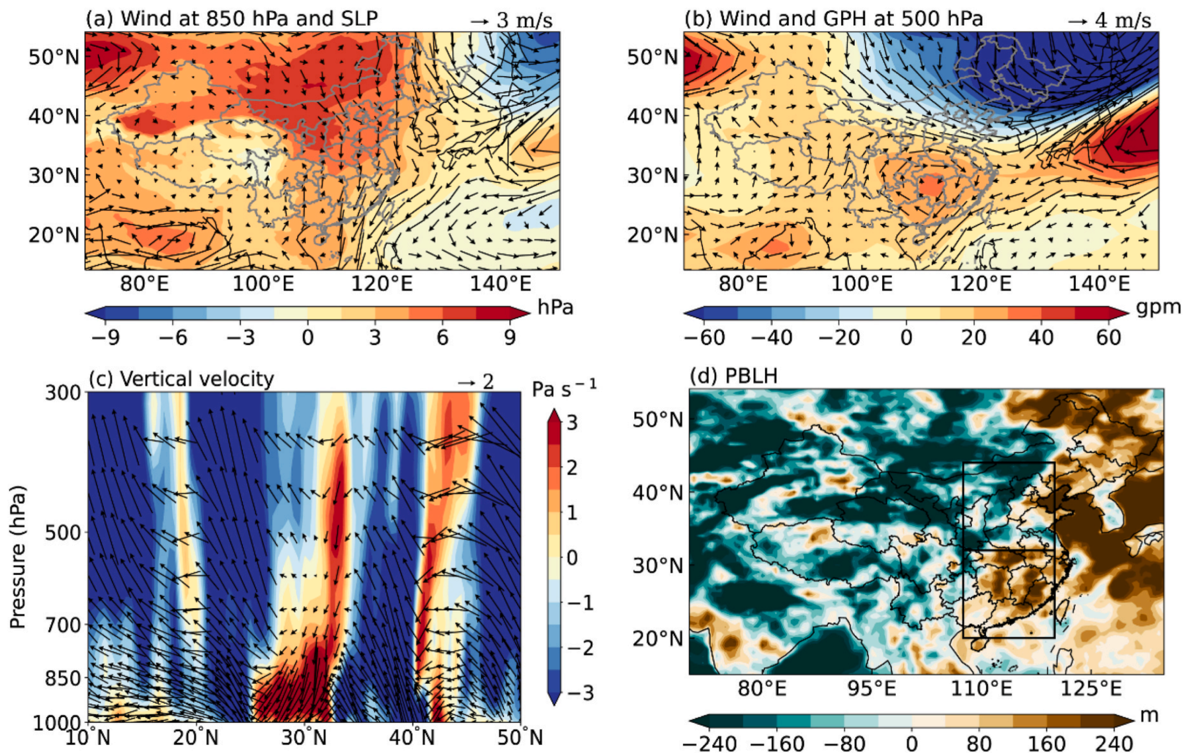

Fig. 6. Composite differences in (a) wind fields (vectors, units: m s^{-1}) at 850 hPa and sea-level pressure (contour, units: hPa), (b) wind fields (vectors, units: m s^{-1}) and geopotential height (contour, units: gpm) at 500 hPa, (c) meridional winds (vectors, units: m s^{-1}) and vertical velocity (contour, units: Pa s^{-1}) averaged over 107.5°–120°E, and (d) planetary boundary layer height (PBLH, units: m), between the strong and weak WPSH days (strong – weak) in July–August 2022. The boxed area marks northern and southern China.

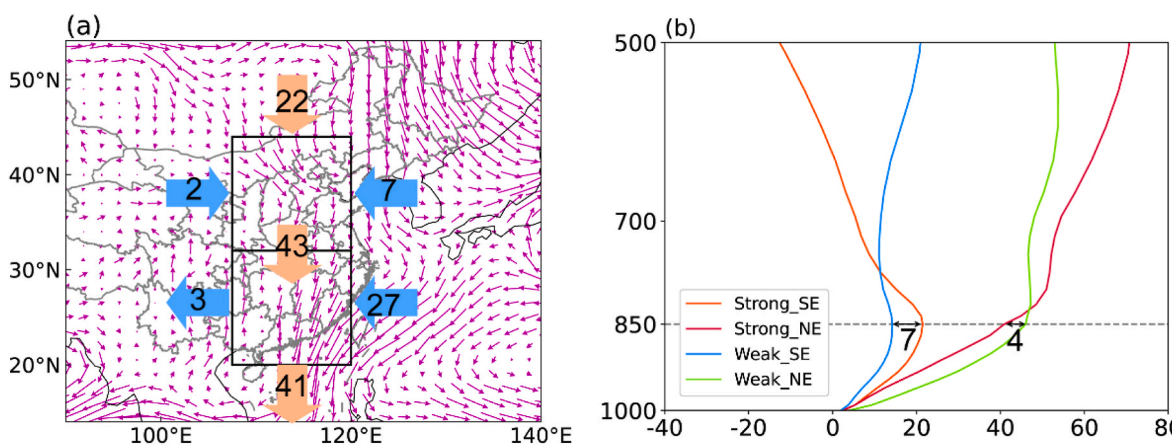

Fig. 7. (a) Composite differences in the horizontal ozone mass fluxes integrated from the surface to 850 hPa along the boundaries between strong and weak WPSH days (units: Gg d^{-1}). (b) Profile of the vertical mass flux over northern China (NC) and southern China (SC) during the strong and weak WPSH days (Units: Gg d^{-1}). The boxed area in (a) marks northern and southern China. Positive values represent downward fluxes, while negative values signify upward fluxes in (b).

2022.

The changes in horizontal ozone mass fluxes from the surface to 850 hPa over southern and northern China simulated by GEOS-Chem model are shown in Fig. 7a. During the strong WPSH days, anomalous northerly winds transport 43 Gg d^{-1} of ozone into southern China from the north, which is largely offset by the export of ozone to the south from southern China (41 Gg d^{-1}). Meanwhile, the anomalous northwesterlies over east of southern China induce an ozone mass gain of 27 Gg d^{-1} due to the weakened winds under the control of high pressure. The profiles of vertical mass flux of ozone during strong and weak WPSH days are given in Fig. 7b. The anomalous downdraft over southern China results in the anomalous downward transport of ozone by about 7 Gg d^{-1} at 850 hPa, contributing to the enhancement of ozone levels in the lower troposphere. In addition, negative anomalies of vertical transport explain the decrease in ozone concentrations between 800 and 500 hPa over southern China.

In northern China, the horizontal transport contributes to an import of 22 Gg d^{-1} of ozone from the north but an export of 43 Gg d^{-1} to the south. The mass flux change of ozone in the east-west direction results in a net ozone increase of 9 Gg d^{-1} during the strong WPSH days relative to weak days. The upward ozone transport at 850 hPa also contributes to the decrease (−4 Gg d^{-1}) in ozone concentration beneath. Overall, horizontal and vertical transport processes contribute to an increase in ozone concentrations over southern China and a decrease in ozone

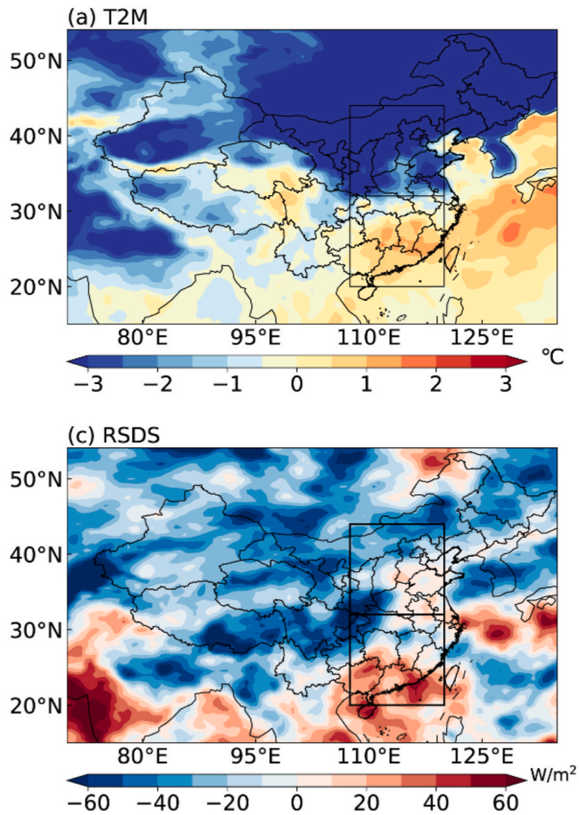

Fig. 8. Composite difference in (a) temperature at 2m (°C), (b) temperature at 850 hPa (°C), (c) downwelling shortwave radiation at the surface (W m^{-2}), and (d) relative humidity at the surface (%) between strong and weak WPSH days. The boxed area marks northern and southern China.

concentrations in northern China in strong WPSH days, relative to the weak WPSH days.

The changes in key meteorological conditions between the strong and weak WPSH days in 2022, which are closely related to the photochemical processes of ozone, are shown in Fig. 8. Compared to the weak WPSH days, southern China exhibits an increase in temperature both at 850 hPa and near the surface during strong WPSH days. Under the control of high-pressure system, the increases in temperature and downwelling shortwave radiation accelerate the photochemical reaction of ozone (Kavassalis and Murphy, 2017), which further increase ozone concentrations over southern China. In contrast, northern China presents a decrease in temperature and, therefore, a reduction in ozone concentrations, likely associated with the anomalous northerly winds bringing cool air from high-latitude regions. Due to the westward-extended position, relative humidity decreases in eastern China during strong WPSH days compared to weak WPSH days (Fig. 8d), which can enhance ozone formation (Yu, 2019) and lead to an increase in ozone concentrations over southern China.

The contributions of net chemical production are calculated using the integrated process rates diagnostic package coupled in GEOS-Chem. The net chemical production of ozone below 850 hPa over southern China is 6.0 Gg d^{-1} higher during strong WPSH days compared to weak days, contributing to the increases in ozone concentrations there. Negative chemical production (−1.5 Gg d^{-1}) over northern China corresponds to lower temperatures, resulting in reduced ozone concentrations during the strong WPSH days relative to weak days.

Note that, the results for 2015–2021 in this study and several recent studies (Zhao and Wang, 2017; Jiang et al., 2020; Mao et al., 2020) found that during strong WPSH episodes, there is an observed rise in ozone levels across northern China, coupled with a reduction in ozone concentrations in the south. This pattern contrasts with the findings for the year 2022. The reason is that the 2022 WPSH is extremely strong in intensity and westward-extended in position compared to the climatology (Fig. 1), with the westward extension ridge even exceeding 80°E (Fig. S4a). During the strong WPSH days in 2022, the whole southern China was dominated by the high pressure. The strongly anomalous anticyclone that induces calm, sunny, hot and dry weather conditions over southern China, favors the production and accumulation of ozone in the lower troposphere. However, during the strong WPSH days in 2015–2021, the center of the anticyclone was located in the western Pacific Ocean (Fig. S4c). It manifested strong southerly winds that bring clean and humid air from ocean to southern China and warm air to northern China, leading to the decreases in ozone concentrations in southern China and increases in northern China. The circulation pattern during weak WPSH days in 2022 is similar to that during strong WPSH days in 2015–2021 (Fig. S4b). Therefore, the unusual synoptic pattern explains the opposite dipole correlation between WPSH and ozone pollution in China in 2022 and that in 2015–2021. This study reveals the significant impact of strong and westward-extended WPSH on ozone concentrations over China, emphasizing the crucial role of the WPSH location in modulating meteorology and air quality.

This finding fills the gap in ozone air quality prediction when the WPSH evolves to a strongly westward-extended scenario. Long-term climate change influences both the intensity and location of the WPSH (Zhou et al., 2009). The location of western edge of WPSH has shifted westward with a trend of 0.14° per year post-1976, accompanied by a strengthening in intensity by 0.18 gpm year^{-1} (Chaluvadi et al., 2021). Although many studies have identified WPSH impacts on meteorological conditions (Li and Zhu, 2010; Mujumdar et al., 2012; Priya et al., 2015; Zhao et al., 2022), the influence of location of WPSH on MDA8 O_3 over China is complex and therefore requires further investigations.

4. Conclusions

In this study, impacts of the unusual WPSH in 2022 on MDA8 O_3 over eastern China are investigated on a synoptic timescale. Compared to climatology, the WPSH was extremely strong and expanded westward during July–August 2022, leading to a prevalent anomalous high-pressure system over East Asia that subsequently influenced ozone levels across China. The observations reveal a significant positive relationship (+0.44) between MDA8 O_3 concentrations and WPSH intensity in southern China, with an increase of by 16.5 μg m^{-3} in MDA8 O_3 concentrations increasing during the strong WPSH days relative to weak WPSH days in 2022. A negative correlation (−0.40) is presented in northern China, with a decrease of 19.0 μg m^{-3} in MDA8 O_3 concentrations. The distinctive dipole pattern of relationship between ozone and WPSH in 2022 contrasts with those from 2015 to 2021 is primarily due to the extremely strong intensity and unique westward-extended location of WPSH in 2022, which created anomalous atmospheric circulation and weather conditions. Specifically, due to the anomalous westward expansion of the WPSH in 2022, southern China, in the center of the anomalous anticyclone, experienced calm, sunny, hot and dry weather conditions along with the large-scale subsidence during the strong WPSH days, resulting in a decrease in horizontal export and an increase in vertical import of ozone. Moreover, high temperatures and low relative humidity over southern China were favorable for ozone photochemical formation. In northern China, strong northerly winds promoted the transport of ozone from northern China to southern China, thereby diminishing ozone during the strong WPSH days. Moreover, negative temperature anomalies suppressed the chemical production of ozone over northern China.

CRediT authorship contribution statement

Mengyun Li: Writing – original draft, Visualization, Software, Methodology, Investigation, Formal analysis, Data curation, Conceptualization. **Yang Yang:** Writing – review & editing, Supervision, Project administration, Formal analysis, Data curation, Conceptualization. **Hailong Wang:** Writing – review & editing. **Pinya Wang:** Writing – review & editing. **Hong Liao:** Writing – review & editing.

Declaration of competing interest

The authors declare that they have no known competing financial interests or personal relationships that could have appeared to influence the work reported in this paper.

Data availability

Data will be made available on request.

Acknowledgments

This work was supported by the National Key Research and Development Program of China (Grant No.: 2020YFA0607803), Jiangsu Science Fund for Distinguished Young Scholars (Grant No.: BK20211541), the Jiangsu Science Fund for Carbon Neutrality (Grant No.: BK20220031), Jiangsu Innovation and Entrepreneurship Team (Grant No.: JSSCTD202346), and Postgraduate Research & Practice Innovation Program of Jiangsu Province (Grant No.: KYCX24_1521). HW acknowledges the support by the U.S. Department of Energy (DOE), Office of Science, Office of Biological and Environmental Research (BER), as part of the Earth and Environmental System Modeling program. The Pacific Northwest National Laboratory (PNNL) is operated for DOE by the Battelle Memorial Institute under contract DE-AC05-76RLO1830.

Appendix A. Supplementary data

Supplementary data to this article can be found online at https://doi.org/10.1016/j.envpol.2024.124515.

References

Chaluvadi, R., Varikoden, H., Mujumdar, M., Ingle, S.T., 2021. Variability of West Pacific subtropical high and its potential importance to the Indian summer monsoon rainfall. Int. J. Climatol. 41 (7), 4047–4060.
Chang, L., Xu, J., Tie, X., Gao, W., 2019. The impact of climate change on the western Pacific subtropical high and the related ozone pollution in Shanghai, China. Sci. Rep. 9 (1), 16998, 16998.
Chen, F., Chen, J., Huang, W., 2021. Weakened East Asian summer monsoon triggers increased precipitation in Northwest China. Sci. China Earth Sci. 64 (5), 835–837.
Choi, W., Kim, K.-Y., 2019. Summertime variability of the western North Pacific subtropical high and its synoptic influences on the East Asian weather. Sci. Rep. 9 (1), 7865.
Colombi, N.K., Jacob, D.J., Yang, L.H., Zhai, S., Shah, V., Grange, S.K., Yantosca, R.M., Kim, S., Liao, H., 2022. Why is ozone in South Korea and the Seoul Metropolitan Area so high and increasing? Atmos. Chem. Phys. 23 (7), 4031–4044.
Dang, R., Liao, H., Fu, Y., 2021. Quantifying the anthropogenic and meteorological influences on summertime surface ozone in China over 2012–2017. Sci. Total Environ. 754, 142394.
David, L.M., Ravishankara, A.R., Brewer, J.F., Sauvage, B., Thouret, V., Venkataramani, S., Sinha, V., 2019. Tropospheric ozone over the Indian subcontinent from 2000 to 2015: data set and simulation using GEOS-Chem chemical transport model. Atmos. Environ. 219, 117039.
Ding, J., Dai, Q., Fan, W., Lu, M., Zhang, Y., Han, S., Feng, Y., 2023. Impacts of meteorology and precursor emission change on O_3 variation in Tianjin, China from 2015 to 2021. J. Environ. Sci. 126, 506–516.
Dong, Y., Li, J., Guo, J., Jiang, Z., Chu, Y., Chang, L., Yang, Y., Liao, H., 2020. The impact of synoptic patterns on summertime ozone pollution in the North China Plain. Sci. Total Environ. 735, 139559.
Feng, Z., Agathokleous, E., Yue, X., Oksanen, E., Paoletti, E., Sase, H., Gandin, A., Koike, T., Calatayud, V., Yuan, X., Liu, X., Marco, A.D., Jolivet, Y., Kontunen-Soppela, S., Hoshika, Y., Saji, H., Li, P., Li, Z., Watanabe, M., Kobayashi, K., 2021. Emerging challenges of ozone impacts on asian plants: actions are needed to protect ecosystem health. Ecosyst. Health Sust. 7 (1), 1911602.
Gao, M., Gao, J., Zhu, B., Kumar, R., Lu, X., Song, S., Zhang, Y., Jia, B., Wang, P., Beig, G., Hu, J., Ying, Q., Zhang, H., Sherman, P., McElroy, M.B., 2020. Ozone pollution over China and India: seasonality and sources. Atmos. Chem. Phys. 20, 4399–4414.
Gong, C., Liao, H., 2019. A typical weather pattern for ozone pollution events in North China. Atmos. Chem. Phys. 19 (22), 13725–13740.
Guan, W., Hu, H., Ren, X., 2019. Sub-seasonal zonal variability of the western Pacific subtropical high in summer: climate impacts and underlying mechanisms. Clim. Dyn. 53, 3325–3344.
He, J., Wang, Y., Hao, J., Shen, L., Wang, L., 2012. Variations of surface O3 in August at a rural site near Shanghai: influences from the West Pacific subtropical high and anthropogenic emissions. Environ. Sci. Pollut. Res. 19, 4016–4029.
Han, H., Liu, J., Shu, L., Wang, T., Yuan, H., 2020. Local and synoptic meteorological influences on daily variability in summertime surface ozone in eastern China. Atmos. Chem. Phys. 20 (1), 203–222.
Hong, M., Shi, J., Zhang, Y., Guo, Z., Qian, L., 2023. Predicting the interannual variability of the subtropical high over the western Pacific Ocean based on the improved information diffusion model. Front. Mar. Sci. 10, 1240768.
Hu, T., Lin, Y., Liu, R., Xu, Y., Ouyang, S., Wang, B., Zhang, Y., Liu, S.C., 2024. What caused large ozone variabilities in three megacity clusters in eastern China during 2015–2020? Atmos. Chem. Phys. 24 (3), 1607–1626.
Jiang, Z., Li, J., Lu, X., Gong, C., Zhang, L., Liao, H., 2020. Impact of western Pacific subtropical high on ozone pollution over eastern China. Atmos. Chem. Phys. 21 (4), 2601–2613.
Kavassalis, S.C., Murphy, J.G., 2017. Understanding ozone-meteorology correlations: a role for dry deposition: ozone-Meteorology Correlations: dry Dep. Geophys. Res. Lett. 44 (6), 2922–2931.
Keller, C.A., Evans, M.J., Knowland, K.E., Hasenkopf, C.A., Modekurty, S., Lucchesi, R.A., Oda, T., Franca, B.B., Mandarino, F.C., Díaz Suárez, M.V., Ryan, R.G., Fakes, L.H., Pawson, S., 2021. Global impact of COVID-19 restrictions on the surface concentrations of nitrogen dioxide and ozone. Atmos. Chem. Phys. 21, 3555–3592.
Li, H., Yang, Y., Jin, J., Wang, H., Li, K., Wang, P., Liao, H., 2023. Climate-driven deterioration of future ozone pollution in Asia predicted by machine learning with multi-source data. Atmos. Chem. Phys. 23 (2), 1131–1145.
Li, J., Zhu, J., 2010. Climatological Features of the Western Pacific Subtropical High southward retreat process in late spring and early summer. Acta. Meteorol. Sinica. 24 (4), 397–412.
Li, K., Jacob, D.J., Liao, H., Zhu, J., Shah, V., Shen, L., Bates, K.H., Zhang, Q., Zhai, S., 2019. A two-pollutant strategy for improving ozone and particulate air quality in China. Nat. Geosci. 12 (11), 906–910.
Li, K., Jacob, D.J., Shen, L., Lu, X., De Smedt, I., Liao, H., 2020. Increases in surface ozone pollution in China from 2013 to 2019: anthropogenic and meteorological influences. Atmos. Chem. Phys. 20 (19), 11423–11433.
Li, M., Yang, Y., Wang, P., Ji, D., Liao, H., 2022. Impacts of strong El Niño on summertime near-surface ozone over China. Atmos. Oceanogr. Sci. Libr. 15 (4), 100193.
Li, M., Yang, Y., Wang, H., Li, H., Wang, P., Liao, H., 2023b. Summertime ozone pollution in China affected by stratospheric quasi-biennial oscillation. Atmos. Chem. Phys. 23 (2), 1533–1544.
Li, X., Hu, Z., Liu, Y., Liang, P., Jha, B., 2023a. Causes and predictions of 2022 extremely hot summer in East Asia. J. Geophys. Res-Atmos. 128 (13), e2022JD038442.

Lin, J.-T., McElroy, M.B., 2010. Impacts of boundary layer mixing on pollutant vertical profiles in the lower troposphere: implications to satellite remote sensing. Atmos. Environ. 44 (14), 1726–1739.
Liu, H., Han, X., Tang, G., Zhang, J., Xia, X., Zhang, M., Meng, L., 2022. Model analysis of vertical exchange of boundary layer ozone and its impact on surface air quality over the North China Plain. Sci. Total Environ. 821, 153436.
Liu, Y., Wang, T., 2020. Worsening urban ozone pollution in China from 2013 to 2017–Part 1: the complex and varying roles of meteorology. Atmos. Chem. Phys. 20 (11), 6305–6321.
Liu, K., Xu, K., Zhu, C., Liu, B., 2022. Diversity of marine heatwaves in the south China sea regulated by ENSO phase. J. Clim. 35, 877–893.
Lo, K.-C., Hung, C.-H., 2015. Forming high ozone concentration in the ambient air of southern taiwan under the effects of western pacific subtropical high. Adv. Meteorol. 2015, 1–14.
Lyu, X.P., Wang, N., Guo, H., Xue, L.K., Jiang, F., Ze, R., Yang, Z., Cheng, H., Cai, Z., Han, L., Zhou, Y., 2019. Causes of a continuous summertime O_3 pollution event in Jinan, a central city in the North China Plain. Atmos. Chem. Phys. 19 (5), 3025–3042.
Ma, Q., Wang, Z., Feng, T., Gao, P., Ma, Y., Yan, P., Feng, G., 2023. Possible influences of spring Barents Sea ice shrinking on Chinese heat wave events. Int. J. Climatol. 43 (13), 6101–6113.
Mao, J., Wang, L., Lu, C., Liu, J., Li, M., Tang, G., Ji, D., Zhang, N., Wang, Y., 2020. Meteorological mechanism for a large-scale persistent severe ozone pollution event over eastern China in 2017. J. Environ. Sci. 92, 187–199.
Mujumdar, M., Preethi, B., Sabin, T.P., Ashok, K., Saeed, S., Pai, D.S., Krishnan, R., 2012. The Asian summer monsoon response to the La Niña event of 2010. Meteorol. Appl. 19 (2), 216–225.
Ni, Y., Yang, Y., Wang, H., Li, H., Li, M., Wang, P., Li, K., Liao, H., 2024. Contrasting changes in ozone during 2019–2021 between eastern and the other regions of China attributed to anthropogenic emissions and meteorological conditions. Sci. Total Environ. 908, 168272.
Ouyang, S., Deng, T., Liu, R., Chen, J., He, G., Leung, J.C.-H., Wang, N., Liu, S.C., 2022. Impact of a subtropical high and a typhoon on a severe ozone pollution episode in the Pearl River Delta, China. Atmos. Chem. Phys. 22 (16), 10751–10767.
Priya, P., Mujumdar, M., Sabin, T.P., Terray, P., Krishnan, R., 2015. Impacts of indo-pacific sea surface temperature anomalies on the summer monsoon circulation and heavy precipitation over northwest India–Pakistan region during 2010. J. Clim. 28 (9), 3714–3730.
Qi, L., He, J., Zhang, Z., Guan, Z., 2010. West Pacific subtropical high double ridges and intraseasonal variability of the South China Sea summer monsoon. Theor. Appl. Climatol. 100, 385–396.
Qu, W., Wang, J., Gao, S., Wu, T., 2013. Effect of the strengthened western Pacific subtropical high on summer visibility decrease over eastern China since 1973. J. Geophys. Res. Atmos. 118 (13), 7142–7156.
Sahu, S.K., Liu, Shuchang, Liu, Song, Ding, D., Xing, J., 2021. Ozone pollution in China: background and transboundary contributions to ozone concentration & related health effects across the country. Sci. Total Environ. 761, 144131.
Shen, L., Liu, J., Zhao, T., Xu, X., Han, H., Wang, H., Shu, Z., 2022. Atmospheric transport drives regional interactions of ozone pollution in China. Sci. Total Environ. 830, 154634.
Shi, Z., Huang, L., Li, J., Ying, Q., Zhang, H., Hu, J., 2020. Sensitivity analysis of the surface ozone and fine particulate matter to meteorological parameters in China. Atmos. Chem. Phys. 20 (21), 13455–13466.
Tan, H.J., Cai, R.-S., Bai, D.P., Hilmi, K., Tonbol, K., 2023. Causes of 2022 summer marine heatwave in the East China Seas. Adv. Clim. Chang. Res. 14 (5), 633–641.
Tang, S., Qiao, S., Wang, B., Liu, F., Feng, T., Yang, J., He, M., Chen, D., Cheng, J., Feng, G., Dong, W., 2023. Linkages of unprecedented 2022 Yangtze River valley heatwaves to Pakistan flood and triple-dip La niña. NPJ Clim. Atmos. Sci. 6 (1), 44.
Wang, N., Huang, X., Xu, J., Wang, T., Tan, Z.-M., Ding, A., 2022. Typhoon-boosted biogenic emission aggravates cross-regional ozone pollution in China. Sci. Adv. 8 (2), eabl6166.
Wang, P., Yang, Y., Li, H., Chen, L., Dang, R., Xue, D., Li, B., Tang, J., Leung, L.R., Liao, H., 2022. North China Plain as a hot spot of ozone pollution exacerbated by extreme high temperatures. Atmos. Chem. Phys. 22 (7), 4705–4719.
Wang, R., Li, Xiao, Ma, H., Li, Xing, Wang, J., Lai, A., 2023. Persistent meteorological drought in the Yangtze River basin during summer–autumn 2022: relay effects of different atmospheric internal variabilities. Atmosphere 14 (9), 1402.
Wang, Y., Hu, H., Ren, X., Yang, X.-Q., Mao, K., 2023. Significant northward jump of the western pacific subtropical high: the interannual variability and mechanisms. J. Geophys. Res-Atmospheres 128 (6), e2022JD037742.
Wu, B., Zhou, T., 2008. Oceanic origin of the interannual and interdecadal variability of the summertime western Pacific subtropical high. Geophys. Res. Lett. 35 (13).
Wu, X., Xu, L., Hong, Y., Chen, Jinfang, Qiu, Y., Hu, B., Hong, Z., Zhang, Y., Liu, T., Chen, Y., Bian, Y., Zhao, G., Chen, Jinsheng, Li, M., 2019. The air pollution governed by subtropical high in a coastal city in Southeast China: formation processes and influencing mechanisms. Sci. Total Environ. 692, 1135–1145.
Wu, L., Wang, C., 2015. Has the western pacific subtropical high extended westward since the late 1970s? J. Clim. 28 (13), 5406–5413.
Yang, Y., Li, M., Wang, H., Li, H., Wang, P., Li, K., Gao, M., Liao, H., 2022. ENSO modulation of summertime tropospheric ozone over China. Environ. Res. Lett. 17 (3), 0304020.
Yang, Y., Zhou, Y., Wang, H., Li, M., Li, H., Wang, P., Yue, X., Li, K., Zhu, J., Liao, H., 2024. Meteorological characteristics of extreme ozone pollution events in China and their future predictions. Atmos. Chem. Phys. 24 (2), 1177–1191.
Yao, M., Hu, Y., Zhang, A., Ji, J.S., Zhao, B., 2022. COPD deaths attributable to ozone in 2019 and future projections using the WHO AQG 2021 in urban China. Eco-Environ. Health. 1 (4), 251–258.
Ye, X., Zhang, L., Wang, X., Lu, X., Jiang, Z., Lu, N., Li, D., Xu, J., 2024. Spatial and temporal variations of surface background ozone in China analyzed with the grid-stretching capability of GEOS-Chem High Performance. Sci. Total Environ. 914, 169909.
Yin, Z., Ma, X., 2020. Meteorological conditions contributed to changes in dominant patterns of summer ozone pollution in Eastern China. Environ. Chem. Lett. 15 (12), 124062.
Yu, S., 2019. Fog geoengineering to abate local ozone pollution at ground level by enhancing air moisture. Environ. Chem. Lett. 17 (1), 565–580.
Zhang, F., Yang, X., Sun, Q., Yao, S., Guo, Q., 2022. Three-dimensional structural anomalies of the western pacific subtropical high ridge and its relationship with precipitation in China during august–september 2021. Atmosphere 13 (7), 1089.
Zhao, Y., Chen, M., Chung, T., Chan, L., Qiu, J., 2023. The 2022 summer marine heatwaves and coral bleaching in China's Greater Bay Area. Mar. Environ. Res. 189, 106044.
Zhao, Y., Cheng, J., Feng, G., Zhi, R., Zheng, Z., Zhang, Z., 2022. Analysis of the atmospheric direct dynamic source for the westerly extended WPSH and record-breaking Plum Rain in 2020. Clim. Dyn. 59 (3), 1233–1251.
Zhao, Z., Wang, Y., 2017. Influence of the West Pacific subtropical high on surface ozone daily variability in summertime over eastern China. Atmos. Environ. 170, 197–204.
Zhou, T., Yu, R., Zhang, J., Drange, H., Cassou, C., Deser, C., Hodson, D.L.R., Sanchez-Gomez, E., Li, J., Keenlyside, N., Xin, X., Okumura, Y., 2009. Why the western pacific subtropical high has extended westward since the late 1970s. J. Clim. 22 (8), 2199–2215.
Zhou, T.-J., 2005. Atmospheric water vapor transport associated with typical anomalous summer rainfall patterns in China. J. Geophys. Res. 110 (D8).
Zhou, Y., Yang, Y., Wang, H., Wang, J., Li, M., Li, H., Wang, P., Zhu, J., Li, K., Liao, H., 2022. Summer ozone pollution in China affected by the intensity of Asian monsoon systems. Sci. Total Environ. 849, 157785.
Zhu, J., Yang, Y., Wang, H., Gao, J., Liu, C., Wang, P., Liao, H., 2024. Impacts of projected changes in sea surface temperature on ozone pollution in China toward carbon neutrality. Sci. Total Environ. 915, 170024.
Zong, L., Yuanjian, Y., Gao, M., Wang, H., Wang, Peng, Wang, P., Wang, P., Zhang, H., Wang, L., Ning, G., Liu, C., Liu, C., Chao, Liu, Li, Y., Gao, Z., 2021. Large-scale synoptic drivers of co-occurring summertime ozone and $PM_{2.5}$ pollution in eastern China. Atmos. Chem. Phys. 21 (11), 9105–9124.